BNL-227967-2025-JAAM

Platinum and Gold Supported on Transition Metal Nitrides for Hydrogen Evolution in an Alkaline Electrolyte

N. N. Nichols, X. Han

To be published in "Energy & Fuels"

March 2025

Chemistry Department

Brookhaven National Laboratory

U.S. Department of Energy

USDOE Office of Science (SC), Basic Energy Sciences (BES)

DISCLAIMER

Platinum and Gold Supported on Transition Metal Nitrides for Hydrogen Evolution in Alkaline Electrolyte

Nathaniel N. Nichols[a], *Xue Han*[b], *Sinwoo Kang*[b], *Hanjun Zhao*[a], *Shyam Kattel*[c], *and Jingguang G. Chen*[a,b]*

[a]Department of Chemical Engineering, Columbia University, New York, NY 10027, USA

[b]Chemistry Division, Brookhaven National Laboratory, Upton, NY 11973, USA

[c]Department of Physics, University of Central Florida, Orlando, FL 32816, USA

*Corresponding Author: jgchen@columbia.edu

Keywords: Transition metal nitrides; Hydrogen evolution reaction; Platinum; Gold; X-ray absorption spectroscopy

ABSTRACT

As the urgency to reduce reliance on fossil fuels increases due to carbon dioxide emissions, hydrogen produced by renewably powered water electrolysis has emerged as a promising technology. Alkaline electrolyzers typically exhibit lower current densities than acidic electrolyzers due to the slow kinetics of the hydrogen evolution reaction (HER) under alkaline conditions. This work developed Pt- and Au-modified transition metal nitride (TMN) thin films for improving alkaline HER kinetics. One monolayer (ML) Pt-VN, Pt-Mo_2N, and Pt-TiN were the most promising thin film catalysts, with alkaline HER activity approaching that of a bulk Pt foil. Additionally, the Gibbs free energy of adsorbed hydrogen was identified as a useful descriptor for alkaline HER activity on TMN and TMN-supported catalysts and has the potential to guide future studies on TMN-based catalysts for enhancing alkaline HER. For practical applications, the thin film catalysts were then extended to Pt- and Au-modified TMN powders for alkaline HER. Both 5 wt.% Pt/TiN and 2 wt.% Pt/TiN powders exhibited lower overpotentials at 5 mA/cm^2 when normalized by Pt electrochemical surface area than the commercial 5 wt.% Pt/C benchmark, suggesting a Pt-TiN synergy that creates opportunities for more cost-effective alkaline HER cathodes. Moreover, 20 wt.% Au/Mo_2N also displayed an enhancement in HER activity when compared to the commercial 20 wt.% Au/C benchmark.

1. INTRODUCTION

Hydrogen is recognized as a source of clean energy in addition to its applications in processing fuels and chemicals, such as petroleum refining, ammonia production, and methanol synthesis.[1,2] New applications in emerging CO_2 conversion processes have also contributed to growing hydrogen demand.[3] However, current methods of hydrogen production have significant carbon footprints, with 95% of hydrogen in the U.S. reportedly produced by steam methane reforming and 4% by coal gasification in 2020.[4] Globally, these carbon-intensive production methods emit 830 million tons of CO_2 annually.[2] Decarbonizing hydrogen production through renewable methods such as water electrolysis powered by carbon-free electricity offers opportunities for addressing future hydrogen demand while reducing carbon footprint.

Water electrolysis uses electricity to drive hydrogen production from water through the cathodic hydrogen evolution reaction (HER), balanced by the oxygen evolution reaction (OER) at the anode. The kinetics of HER in acidic environments are faster due to the rapid formation of hydrogen intermediates from H_3O^+,[5] but the corrosive environment of acidic water electrolysis requires components such as electrodes and bipolar plates to be manufactured with materials containing rare and expensive elements such as Pt, Au, and Ir.[6] Alternatively, alkaline electrolyzers can be manufactured from Earth-abundant materials such as Ni and stainless steel, making them more cost-effective.[6] Currently, Ni-based catalysts are the state of the art for alkaline HER but suffer from low current densities that lead to larger electrolyzer stacks and space requirements. Although Pt exhibits higher current densities for alkaline HER than Ni,[7] the Pt loading needs to be significantly reduced.[8–10]

Transition metal nitrides (TMNs) are promising catalytic supports because the electronic properties of TMNs are often similar to those of Pt-group metals, offering the potential to support

a low coverage of Pt while maintaining HER activity similar to bulk Pt.[11] One study by Mou et al. showed that depositing one monolayer (ML) of Pt on a WN film demonstrated a similar HER activity to that of a bulk Pt film in acidic conditions.[12] Meanwhile, the same study found that the Gibbs free energy of adsorbed hydrogen (ΔG_H) on TMNs can be used as a descriptor for acidic HER activity on TMN films.[12] ΔG_H is often used as a descriptor of HER activity because the adsorption of hydrogen atoms appears in all three steps of the Volmer-Tafel-Heyrovsky HER mechanism.[13]

In this work, TMN thin films of Ti, Mo, W, V, and Ta were synthesized and then modified with Pt and Au. While Pt shows excellent HER activity, Au was also investigated to elucidate if TMNs can enhance the alkaline HER performance of other precious metals. The film electrocatalysts were tested to obtain exchange current densities ($\log_{10}(i_0)$) that were used to quantify alkaline HER activity. The activity was then correlated with ΔG_H from density functional theory (DFT) calculations that yielded a volcano-type relationship. The shape of the plot emerged due to the unmodified TMNs binding hydrogen too strongly while the Au-modified TMNs bind hydrogen too weakly, both of which decreased alkaline HER activity. ΔG_H was therefore revealed to be a descriptor of alkaline HER activity for TMN-based catalysts, with Pt-modified TMNs exhibiting the highest alkaline HER activity due to an ideal binding strength of hydrogen. The results from thin films were then extended to more practical powder catalysts. To determine the oxidation states of Pt and Au under alkaline HER conditions, the powder catalysts were further characterized using *in-situ* X-ray absorption spectroscopy (XAS).

2. METHODS

2.1. TMN Thin Film and Powder Synthesis and Characterization. TMN thin films of Ti, Mo, W, V, and Ta, were synthesized according to previously published methods.[12] As reported

previously, the composition and structure of the TMN thin films were analyzed using glancing incidence X-ray diffraction spectroscopy (GI-XRD) at an X-ray incident angle of 1°. GI-XRD revealed the formation TMN thin films, and the results were consistent with previously published studies of TMNs (Figure S1).[12] Based on the results of GI-XRD characterization, the TMNs in this study will be referred to as: VN, Ta_3N_5, WN, Mo_2N, and TiN. The TMN thin films were modified with ML of Pt or Au using physical vapor deposition (PVD).[12,14–16] After modifying these TMN films with Pt and Au overlayers, the films were again characterized by GI-XRD and the results were found to be consistent with other published data (Figure S2).[12] XPS analysis confirmed the presence of Pt and Au on the surface of the TMN films after PVD (Figure S3). Additionally, all the TMN films exhibited XPS peaks corresponding to their respective TMNs indicating that TMNs were present at the surface of the films. The XPS spectra of the TMN thin films in this study were also consistent with previously published work.[12,17–23]

TiN powder was synthesized according to previously published methods.[12,24] Mo_2N powder was synthesized by first heating ammonium paramolybdate in a muffle furnace for 4 hours at 500 °C. Then the same procedure that was used for the metal foils was employed except that the temperature was held at 750 °C for 2 hours. Incipient wetness impregnation (IWI) was used to synthesize 5 wt.% and 2 wt.% Pt-modified TiN powders and 20 wt.% and 5 wt.% Au-modified Mo_2N powders.

2.2. Powder Catalyst Electrode Preparation and Characterization. Powder catalyst electrodes with 0.5 mg of catalyst per geometric cm^2 were prepared according to previously published methods.[12] Commercial 5 wt.% Pt-modified and 20 wt.% Au-modified Vulcan XC-72 carbon powders (Premetek Co.) were used as benchmark catalysts. The electrochemical surface area (ECSA) of the Pt-modified powder electrodes were quantified using copper-stripping.[12,25,26]

For Au-modified powder electrodes, the copper-stripping method for determining ECSA could not be performed on the Au/Mo_2N powder catalysts due to the poor electrochemical stability of Mo_2N in oxidative environments.[12] Other methods for measuring ECSA such as double layer capacitance, CO stripping, and AuO CV peak analysis were also unable to accurately measure the ECSA for the Au/Mo_2N powders. Therefore, the electrochemical results of Au-modified electrodes were normalized by the geometric surface area.

2.3. Electrochemical Activity and Stability Measurements. Electrochemical activity measurements were performed in a three-electrode electrochemical cell set-up using previously described methods except that an alkaline (0.1 M KOH) electrolyte was used.[12,27,28] Turn over frequency (TOF) analysis was also performed on the Pt-modified catalysts by employing previously published methods.[12,29] To test the stability of the powder catalyst samples, two-hour chronopotentiometry (CP) measurements were performed at -5 mA/cm^2_{ECSA} for the Pt-modified catalysts and -5 mA/cm^2_{geo} for the Au-modified catalysts.

2.4. *In-situ* X-ray Absorption Spectroscopy Measurements. *In-situ* X-ray absorption spectra were measured at the 7-BM beamline of the National Synchrotron Light Source II at Brookhaven National Laboratory. The *in-situ* data was collected using previously described methods in 0.1 M KOH electrolyte.[12,30–32]

3. RESULTS AND DISCUSSION

3.1. Alkaline HER Activity of TMN and Metal-modified TMN Thin Films. The alkaline HER performance of unmodified Ta_3N_5, TiN, VN, WN, and Mo_2N, as well as Pt-modified and Au-modified thin films of these TMNs, was compared through LSV measurements. In Figure 1a, none of the unmodified TMNs exhibited lower overpotentials than Pt; however, WN and Mo_2N displayed lower overpotentials than bulk Au. Among all the unmodified TMNs, WN performed

the best requiring slightly above -0.45 V vs. RHE (hereafter all potentials will be reported as vs. RHE) to achieve a current density of -10 mA/cm$^2_{geo}$. After modifying the TMNs with Pt (Figure 1b), 1 ML Pt-VN, 1 ML Pt-Mo_2N, 1 ML Pt-TiN, and 1 ML Pt-Ta_3N_5 showed improved performance compared to their unmodified counterparts. 1 ML Pt-VN exhibited an especially improved performance by achieving a current density of -10 mA/cm$^2_{geo}$ at slightly above -0.2 V, similar to that of bulk Pt. The results reveal that by modifying TMNs with 1 ML coverage of Pt, their alkaline HER activity can approach that of bulk Pt.

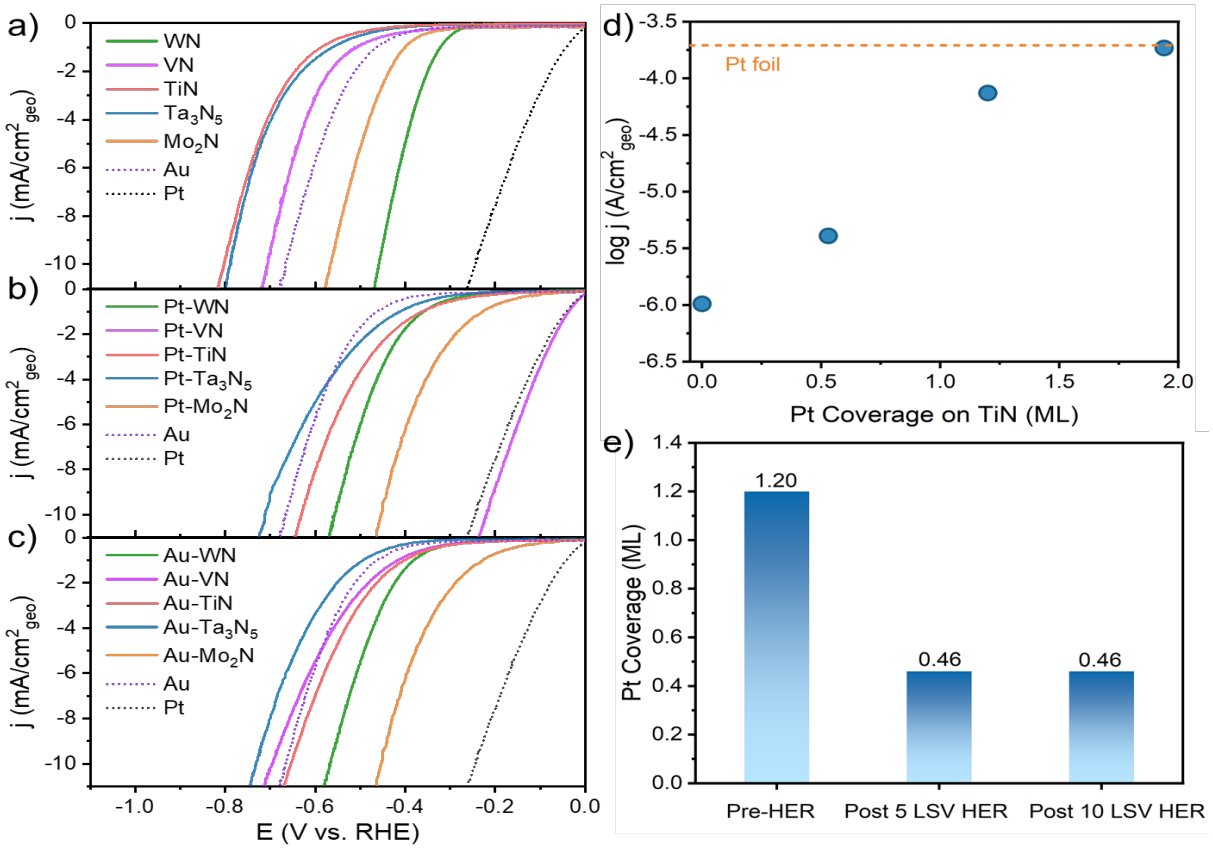

Figure 1. Alkaline HER LSV curves for unmodified TMNs (a), Pt-modified TMNs (b), and Au-modified TMNs (c) in H_2-saturated 0.1 M KOH. The dashed lines represent the bulk metals, while the solid lines represent the TMN-based thin films. (d) Alkaline HER activity quantified by

$\log_{10}(i_0)$ as a function of Pt coverage on TiN thin films and (e) Pt overlayer coverages before LSV testing, after 5 LSV scans, and after 10 LSV scans of alkaline HER testing for Pt-modified TiN.

In Figure 1c, none of the Au-modified TMN thin films showed lower overpotentials than bulk Pt foil for alkaline HER. However, 1 ML Au-Mo_2N and 1 ML Au-WN had lower overpotentials than bulk Au foil at -10 mA/cm^2_{geo}. The 1 ML Au-Mo_2N catalyst exhibited an especially enhanced performance compared to Mo_2N. The overpotential decreased from -0.57 V for Mo_2N to -0.45 V for 1 ML Au-Mo_2N at -10 mA/cm^2_{geo}.

The relationship between Pt coverage on TMNs and alkaline HER activity was investigated and exemplified by using Pt-modified TiN thin films with different Pt coverages (Figure 1d). HER activity, represented by the value of $\log_{10}(i_0)$, increased with Pt coverage on TiN. Additionally, modifying TiN with a Pt coverage of two ML led to an alkaline HER activity that matched the activity of bulk Pt. A similar phenomena was also observed in prior work on Pt-modified WN and NbN.[33] These results indicate that Pt loadings can be reduced to the ML scale on TMNs and thereby potentially decrease catalyst cost by orders of magnitude.[10]

The stability of the Pt overlayer on the TiN film sample was also investigated. The overlayer thickness of Pt on the TiN film, calculated from XPS, before LSV testing, after 5 LSV scans, and after 10 LSV scans is shown in Figure 1e. After 5 LSV scans in alkaline conditions, the Pt overlayer on TiN decreased significantly. However, after 5 more LSV scans, the Pt overlayer did not decrease further on TiN. The decrease in the Pt overlayer was likely due to Pt agglomeration because Pt dissolution would lead to a further decrease of Pt coverage from 5 to 10 LSV scans. Similar agglomeration was also observed in previous studies with Pt-modified TMC thin films.[34]

3.2. Correlation between Alkaline HER Activity and ΔG_H. To elucidate if ΔG_H can be used as a descriptor for alkaline HER activity on TMN based catalysts, the $\log_{10}(i_0)$ for each thin film

catalyst was plotted against their respective DFT-calculated ΔG_H values reported in a previous publication (Figure 2).[12] DFT calculations were performed using the Vienna Ab Initio Simulation Package (VASP).[35,36] The bulk structures of MoN, TaN, TiN, and VN were modeled as cubic structures and bulk phase WN was modeled using a hexagonal closed pack structure. All calculations were completed for (111) surfaces except MoN and WN, which utilized (001) surfaces.

The volcano-like shape of Figure 2 is due to the unmodified TMNs binding hydrogen too strongly and the bulk Au and Au-modified TMNs binding hydrogen too weakly, both of which correspond to a decrease in alkaline HER activity. Alkaline HER activity is therefore maximized at a ΔG_H, similar to that of bulk Pt. The results in Figure 2 indicate that ΔG_H can be used as a descriptor of alkaline HER activity on TMN based catalysts.

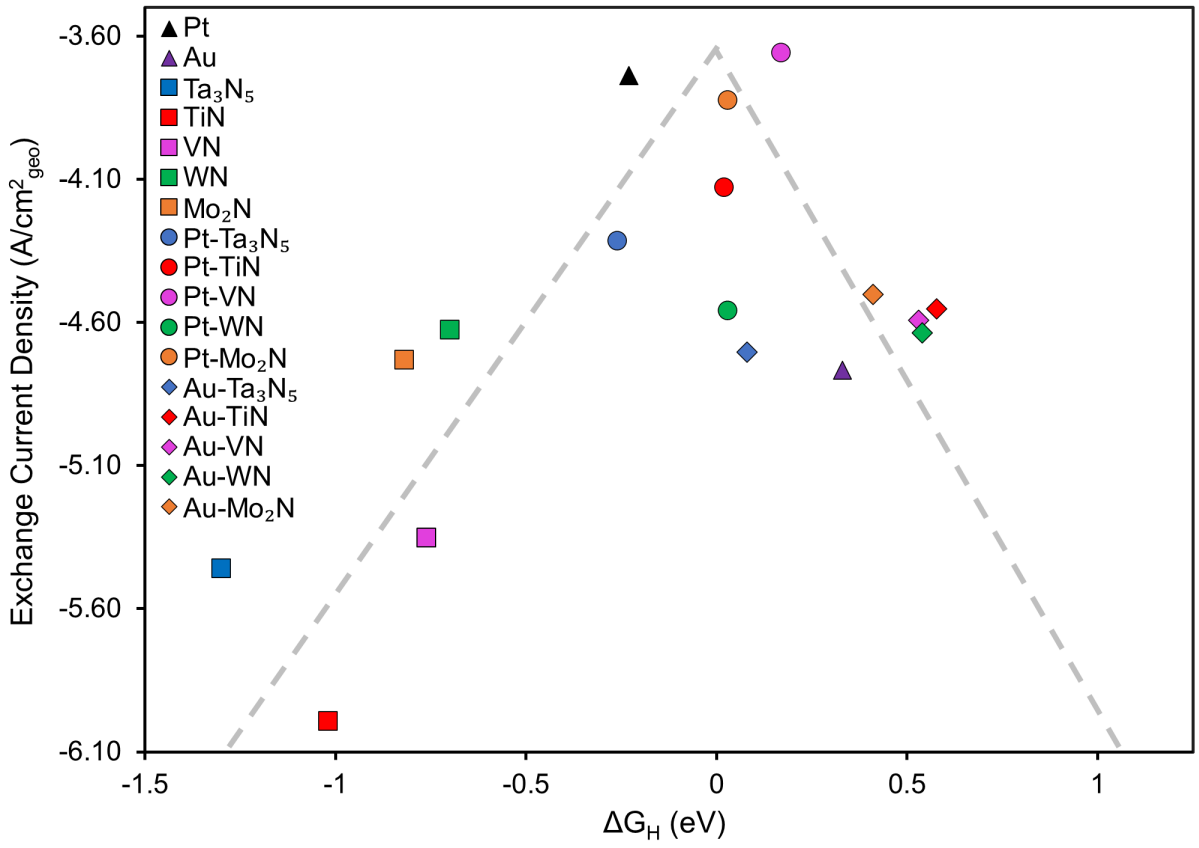

Figure 2. Volcano plot comparing $\log_{10}(i_0)$ for thin films versus calculated ΔG_H for unmodified TMNs, Pt-modified TMNs, Au-modified TMNs, and monometallic metals. Dashed lines are drawn to guide the eyes. ΔG_H values were obtained from a previous publication.[12]

3.3. Extension of Thin Film Results to Powder Catalysts. The results of the thin film catalysts were then extended to more practical Pt- and Au-modified TMN powders for alkaline HER. Based on the thin film results, Pt/TiN and Au/Mo_2N were selected due to their relatively high HER activity among the Pt/TMN and Au/TMN catalysts, respectively. After synthesizing the TMN powders, XRD confirmed that the TiN and Mo_2N powders consisted of only single-phase TiN and Mo_2N, respectively (Figures S4-5). The weight loadings of Pt on TiN and Au on Mo_2N were confirmed using inductively coupled plasma optical emission spectroscopy (ICP-OES) (Tables S3-4). Transmission electron microscopy (TEM) and Cu-stripping measurements revealed the average Pt particle sizes and ECSAs of the Pt/TiN and commercial Pt/C powders were similar to previously published data (Figure S6 and Table S5).[12] The TEM results of the Au-based catalysts indicated that the Au/Mo_2N and commercial Au/C powders had a similar particle size distribution between 2-4 nm.

The Pt/TiN and Au/Mo_2N powder catalysts were tested to validate the trends in alkaline HER from the corresponding thin film catalysts. The normalized LSV curves (Figure 3b) showed that the 5% Pt/TiN powder reached a current density of 5 mA/cm^2_{ECSA} at -0.16 V and outperformed the benchmark 5% Pt/C powder. When further decreasing the Pt loading to 2% Pt/TiN, the TiN-based catalyst was still able to outperform the benchmark 5% Pt/C by reaching a current density of 5 mA/cm^2_{ECSA} at -0.18 V, revealing a synergy between TiN and Pt that enables enhanced HER activity. Furthermore, turnover frequency (TOF) analysis revealed that 5% Pt/TiN also exhibited a higher TOF than 5% Pt/C (Figure S7). The 1 ML Pt-TiN thin film likely did not perform as well

for alkaline HER as compared to the powders due to the weaker interaction between Pt and TiN when using PVD compared to IWI.

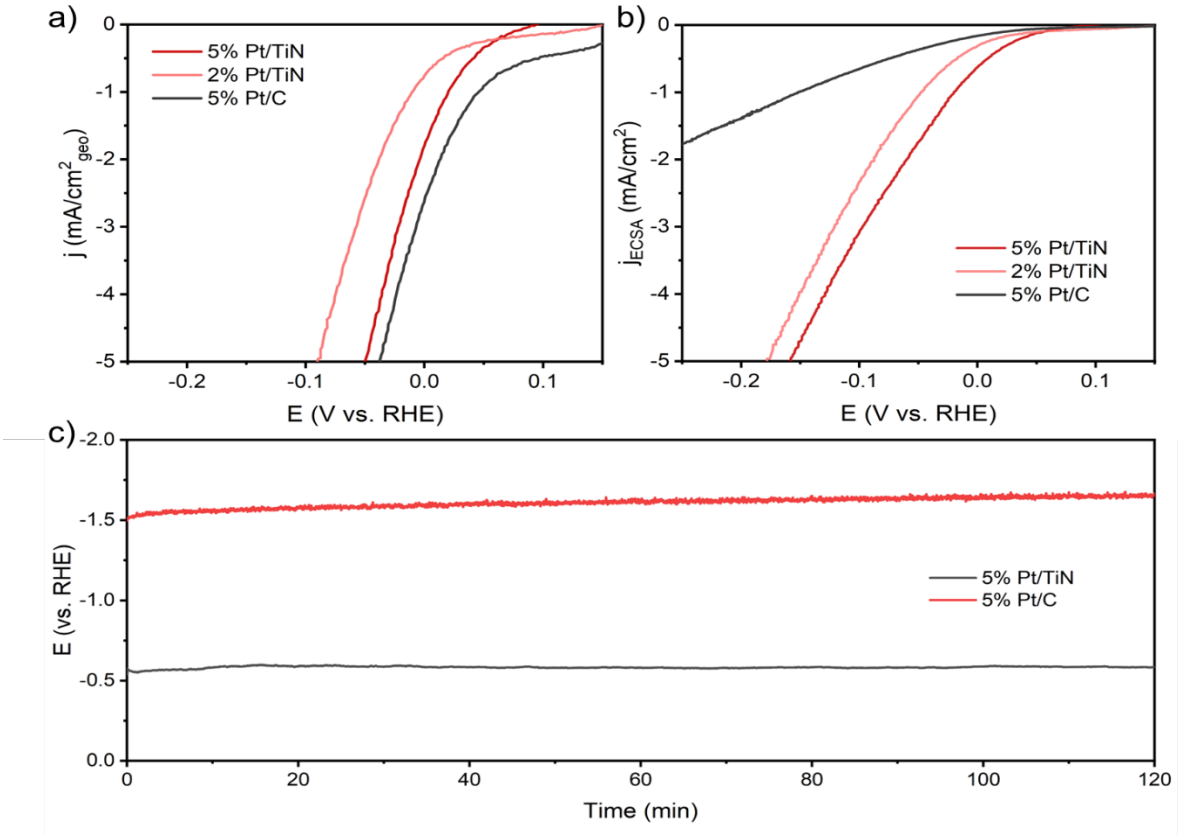

Figure 3. Alkaline HER LSV curves normalized by geometric surface area (a) and ECSA (b) for 5% and 2% Pt/TiN and commercial 5% Pt/C powders in 0.1 M KOH. (c) Two-hour alkaline HER stability tests at -5 mA/cm^2_{ECSA} for 5% Pt/TiN and commercial 5% Pt/C powders in 0.1 M KOH.

The stability of the 5% Pt/TiN powder catalyst was also investigated. After two hours of stability testing at -5 mA/cm^2_{ECSA} in alkaline conditions, 5% Pt/TiN still displayed a lower overpotential than commercial 5% Pt/C (Figure 3c). The 5% Pt/TiN catalyst showed a stable overpotential after two hours while the overpotential for 5% Pt/C increased throughout the two-hour stability test. Furthermore, compared to the stability of the 1 ML Pt-TiN thin film, 5% Pt/TiN powder required

approximately 0.4 V less overpotential to reach the same geometric current density, thereby highlighting the utility of powders over their thin film counterparts for practical applications (Figure S11).

Au/Mo_2N powders were tested to elucidate if the enhanced alkaline HER activity of Au-modified Mo_2N films could be extended to powder catalysts (Figure 4a). The geometrically normalized LSV results show that 20% Au/Mo_2N exhibited an overpotential of -0.28 V at a current density of -5 mA/cm^2_{geo} which was lower than that of commercial 20% Au/C (-0.36 V). In addition, 5% Au/Mo_2N exhibited similar alkaline HER performance to 20% Au/C. The Au-modified powder results follow a similar trend to the Au-modified thin films, which further highlights that thin films can be used as model systems for designing practical powder catalysts.

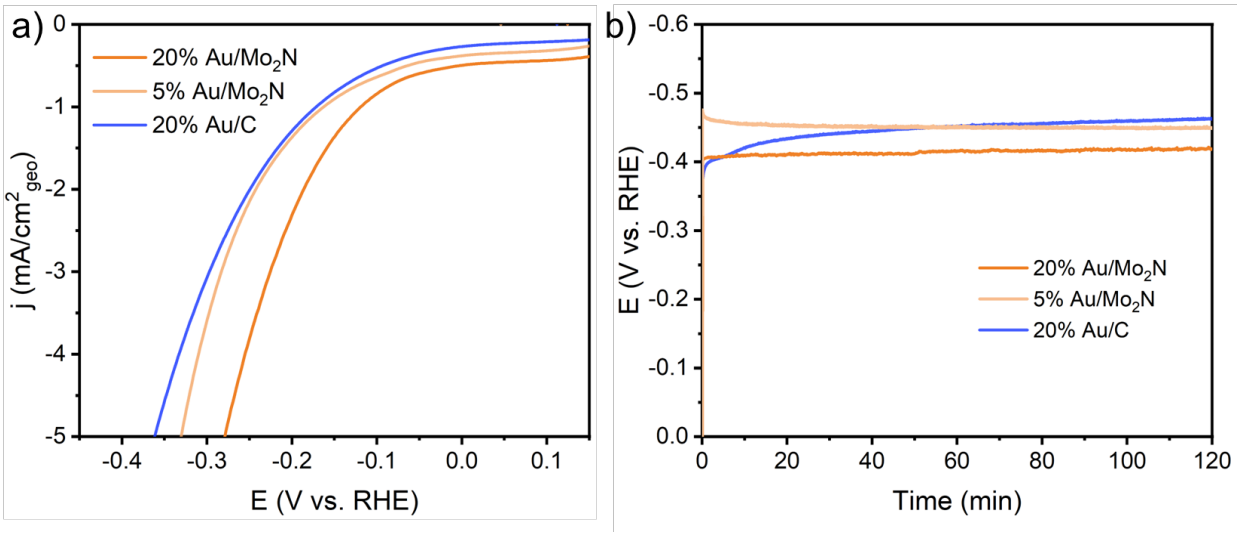

Figure 4. Alkaline HER LSV curves normalized by geometric surface area (a) and two-hour stability test at -5 mA/cm^2_{geo} (b) for 20% and 5% Au/Mo_2N and commercial 20% Au/C powders in 0.1 M KOH.

The Au/Mo_2N powder catalysts were further evaluated through a two-hour stability test at -5 mA/cm^2_{geo} (Figure 5b). After two hours, both 20% Au/Mo_2N and 5% Au/Mo_2N exhibited lower overpotentials than 20% Au/C, confirming the electrochemical stability of the Au/Mo_2N catalysts.

3.4. *In-situ* X-ray Absorption Spectroscopy Characterization. *In-situ* XAS was used to investigate the chemical states of Pt and Au during alkaline HER. As shown in Figure 5a, Pt L_3-edge X-ray absorption near edge structure (XANES) spectra for 5% Pt/TiN revealed that the white line peaks at different applied potentials, from OCP to -0.2 V, were the same as the Pt foil, indicating that Pt remained in a metallic state under alkaline HER conditions.[12] Similarly, the white line peak in the Au L_3-edge XANES spectra (Figure 5b) of 5% Au/Mo_2N also showed metallic Au during alkaline HER. Overall, the *in-situ* XANES results revealed Pt and Au both remained in their respective metallic states during the reduction process. Since Pt and Au maintained their metallic states under reaction conditions, this work further demonstrates that simplified thin-film catalysts and DFT models, which utilize metallic Pt and Au, can be used to guide and inform electrocatalyst design.

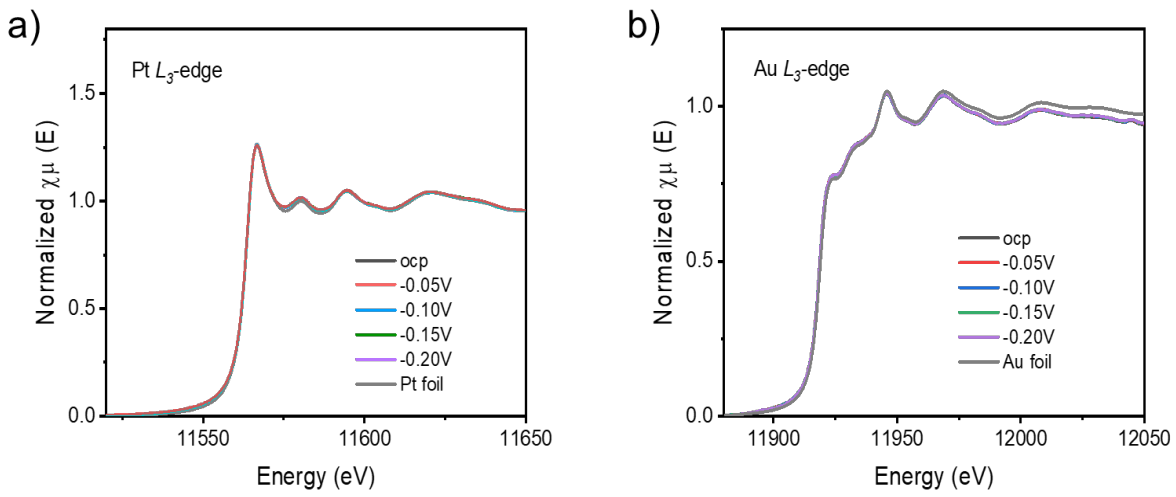

Figure 5. In-situ XANES characterization of (a) 5% Pt/TiN and (b) 5% Au/Mo_2N powder catalysts.

4. CONCLUSIONS

In summary, unmodified nitride films of Ti, Mo, W, V, and Ta and Pt- and Au-modified TMN films were synthesized and their alkaline HER activity were compared to bulk Pt and Au foils. The results showed that depositing one ML of Pt on TMN films significantly enhanced the alkaline HER activity. The coverage of Pt on TiN was also varied and revealed that the alkaline HER activity of two ML of Pt on TiN matched bulk Pt foil. In addition to the Pt-modified TMN films, 1 ML Au-Mo_2N showed higher HER activity than bulk Au. Plotting the exchange current density, $\log_{10}(i_0)$, for each film against their ΔG_H calculated from DFT established ΔG_H as a descriptor for alkaline HER activity on TMN based catalysts. Encouraged by the promising thin film results, powder catalysts were synthesized and tested for alkaline HER. Both 5% Pt/TiN and 2% Pt/TiN powder catalysts outperformed the benchmark 5% Pt/C. Similarly, 20% Au/Mo_2N outperformed the benchmark of 20% Au/C catalyst for alkaline HER. These findings highlight the opportunities for reducing precious metal loading while maintaining HER activity, thereby increasing the

prospects of alkaline HER for commercial applications.[10] The trend established in this work can also be used to guide the future development of TMN-based catalysts for alkaline HER. Despite the potential differences in the morphology and structures between thin films and powder catalysts, it is encouraging to observe the similar trends in the HER activity of these two types of model and practical catalysts, demonstrating the possibility of using model surfaces to identify active HER catalysts with lower precious metal loadings.

ASSOCIATED CONTENT

Supporting Information.

The following files are available free of charge.

XRD and XPS spectra of thin films; previously published predicted ΔG_H; measured $\log_{10}(i_0)$ of thin films; XRD spectra of powders; measured ICP-OES metal loadings of powders; measured ECSA values of Pt-modified powders; TEM images of powders; TOF plot (PDF)

AUTHOR INFORMATION

Corresponding Author

Jingguang G. Chen – Department of Chemical Engineering, Columbia University, New York, NY 10027, USA; Chemistry Division, Brookhaven National Laboratory, Upton, NY 11973, USA; Email: jgchen@columbia.edu

Authors

Nathaniel N. Nichols – Department of Chemical Engineering, Columbia University, New York, NY 10027, USA

Xue Han – Chemistry Division, Brookhaven National Laboratory, Upton, NY 11973, USA

Sinwoo Kang – Chemistry Division, Brookhaven National Laboratory, Upton, NY 11973, USA

Hanjun Zhao – Department of Chemical Engineering, Columbia University, New York, NY 10027, USA

Shyam Kattel – Department of Physics, University of Central Florida, Orlando, FL 32816, USA

Author Contributions

Nathaniel N. Nichols: conceptualization, methodology, investigation, writing—original draft, and writing—review & editing. Xue Han: investigation and writing—review & editing. Sinwoo Kang: investigation and writing—review & editing. Hanjun Zhao: investigation. Shyam Kattel: writing––review & editing. Jingguang G. Chen: conceptualization, methodology, writing—review & editing, funding acquisition, and supervision.

Notes

The authors declare no competing financial interest.

ACKNOWLEDGMENTS

This work was financially supported by the U.S. Department of Energy, Office of Basic Energy Sciences, Chemical Sciences, Geosciences, and Biosciences Division (DE-SC00234430). This research used the resources of the Center for Functional Nanomaterials (CFN) and beamlines 7-BM (QAS) of the National Synchrotron Light Source II (NSLS-II) at Brookhaven National Laboratory (contract nos. DE-SC0012704 and DE-SC0012653), US DOE Office of Science User Facilities. Beamline operations were supported in part by the Synchrotron Catalysis Consortium (US DOE, Office of Basic Energy Sciences, grant no. DE-SC0012335). We thank Dario Lewczyk and Prof. Peter Khalifah for preparing some of the TMN films.

REFERENCES

1. Tackett, B. M.; Sheng, W.; Chen, J. G. Opportunities and Challenges in Utilizing Metal Modified Transition Metal Carbides as Low-Cost Electrocatalysts. *Joule* **2017**, *1* (2), 253–263. DOI: 10.1016/j.joule.2017.07.002
2. International Energy Agency. *The Future of Hydrogen: Seizing Today's Opportunities*; IEA: Paris, 2019; https://www.iea.org/reports/the-future-of-hydrogen (accessed 2023-08-16).
3. Porosoff, M. D.; Yan, B.; Chen, J. G. Catalytic Reduction of CO2 by H2 for Synthesis of CO, Methanol and Hydrocarbons: Challenges and Opportunities. *Energy Environ. Sci.* **2016**, *9* (1), 62–73. DOI: 10.1039/C5EE02657A
4. U.S. Department of Energy, Office of Fossil Energy. *Hydrogen Strategy: Enabling a Low-Carbon Economy*; 2020; https://www.energy.gov/sites/prod/files/2020/07/f76/USDOE_FE_Hydrogen_Strategy_July2020.pdf (accessed 2023-08-14).
5. Bao, F.; Kemppainen, E.; Dorbandt, I.; Bors, R.; Xi, F.; Schlatmann, R.; van de Krol, R.; Calnan, S. Understanding the Hydrogen Evolution Reaction Kinetics of Electrodeposited Nickel-Molybdenum in Acidic, Near-Neutral, and Alkaline Conditions. *ChemElectroChem* **2021**, *8* (1), 195–208. DOI: 10.1002/celc.202001436
6. Kumar, S.S.; Lim, H. An Overview of Water Electrolysis Technologies for Green Hydrogen Production. *Energy Reports* **2022**, *8*, 13793-13813. DOI: 10.1016/j.egyr.2022.10.127
7. Xing, Z.; Gan, L.; Wang, J.; Yang, X. Experimental and Theoretical Insights into Sustained Water Splitting with an Electrodeposited Nanoporous Nickel Hydroxide@nickel Film as an Electrocatalyst. *J. Mater. Chem. A* **2017**, *5* (17), 7744–7748. DOI: 10.1039/C7TA01907F
8. London Metal Exchange. *LME Nickel Market Data and Information*; https://www.lme.com/Metals/Non-ferrous/LME-Nickel (accessed 2023-08-24).
9. London Metal Exchange. *LBMA Platinum Market Data and Information*; https://www.lme.com/Metals/Precious/LBMA-Platinum (accessed 2023-08-24).
10. Esposito, D.V.; Chen, J.G. Monolayer Platinum Supported on Tungsten Carbides as Low-Cost Electrocatalysts: Opportunities and Limitations. *Energy Environ. Sci.* **2011**, *4* (10), 3900–3912. DOI: 10.1039/C1EE01851E
11. Chen, J. G. Carbide and Nitride Overlayers on Early Transition Metal Surfaces: Preparation, Characterization, and Reactivities. *Chem. Rev.* **1996**, *96* (4), 1477–1498. DOI: 10.1021/cr950232u
12. Mou, H.; Jeong, J. J.; Lamichhane, B.; Kattel, S.; Zhuang, Z.; Lee, J. H.; Chang, Q.; Chen, J. G. Trends in Electrocatalytic Activity and Stability of Transition-Metal Nitrides. *Chem Catal.* **2024**, *4* (2), 100867. DOI: 10.1016/j.checat.2023.100867
13. Zhu, Y.; Li, L.; Cheng, H.; Ma, J. Alkaline Hydrogen Evolution Reaction Electrocatalysts for Anion Exchange Membrane Water Electrolyzers: Progress and Perspective. *JACS Au* **2024**, *4* (12), 4639–4654. DOI: 10.1021/jacsau.4c00898
14. Westwood, W. D. Physical Vapor Deposition. In *Microelectronic Materials and Processes*; Levy, R. A., Ed.; NATO ASI Series; Springer Netherlands: Dordrecht, 1989; pp 133–201. DOI: 10.1007/978-94-009-0917-5_4

15. Cumpson, P. J.; Seah, M. P. Elastic Scattering Corrections in AES and XPS. II. Estimating Attenuation Lengths and Conditions Required for Their Valid Use in Overlayer/Substrate Experiments. *Surf. Interface Anal.* **1997**, *25* (6), 430–446. DOI: 10.1002/(SICI)1096-9918(199706)25:6<430::AID-SIA254>3.0.CO;2-7.
16. Esposito, D. V.; Hunt, S. T.; Kimmel, Y. C.; Chen, J. G. A New Class of Electrocatalysts for Hydrogen Production from Water Electrolysis: Metal Monolayers Supported on Low-Cost Transition Metal Carbides. *J. Am. Chem. Soc.* **2012**, *134* (6), 3025–3033. DOI: 10.1021/ja208656v
17. Liu, J.; Tang, S.; Lu, Y.; Cai, G.; Liang, S.; Wang, W.; Chen, X. Synthesis of Mo2N Nanolayer Coated MoO2 Hollow Nanostructures as High-Performance Anode Materials for Lithium-Ion Batteries. *Energy Environ. Sci.* **2013**, *6* (9), 2691–2697. DOI: 10.1039/C3EE41006D
18. Glaser, A.; Surnev, S.; Netzer, F. P.; Fateh, N.; Fontalvo, G. A.; Mitterer, C. Oxidation of Vanadium Nitride and Titanium Nitride Coatings. *Surf. Sci.* **2007**, *601* (4), 1153–1159. DOI: 10.1016/j.susc.2006.12.010
19. Zhao, Y.; Liu, Y.; Cao, H.; Ye, J.; Gao, S.; Tu, M. Synthesis of VN Nanopowders by Thermal Nitridation of the Precursor and Their Characterization. *J. Alloys Compd.* **2008**, *464* (1–2), 75–80. DOI: 10.1016/j.jallcom.2007.09.068
20. Lin, D.H.; Chang, K.-S. Photocatalytic and Photoelectrochemical Performance of Ta3N5 Microcolumn Films Fabricated Using Facile Reactive Sputtering. *J. Appl. Phys.* **2016**, *120* (7), 075303. DOI: 10.1063/1.4960806
21. Wen, M.; Meng, Q. N.; Yu, W. X.; Zheng, W. T.; Mao, S. X.; Hua, M. J. Growth, Stress and Hardness of Reactively Sputtered Tungsten Nitride Thin Films. *Surf. Coat. Technol.* **2010**, *205* (7), 1953–1961. DOI: 10.1016/j.surfcoat.2010.08.082
22. Kim, J. B.; Nandi, D. K.; Kim, T. H.; Jang, Y.; Bae, J.S.; Hong, T. E.; Kim, S.H. Atomic Layer Deposition of WNx Thin Films Using a F-Free Tungsten Metal-Organic Precursor and NH3 Plasma as a Cu-Diffusion Barrier. *Thin Solid Films* **2019**, *685*, 393–401. DOI: 10.1016/j.tsf.2019.06.051
23. Moulder, J.F.; Stickle, W.F.; Sobol, P.E.; Bomben, K.D. *Handbook of X-Ray Photoelectron Spectroscopy*; Perkin-Elmer Corporation, 1992.
24. Choi, D.; Kumta, P. N. Nanocrystalline TiN Derived by a Two-Step Halide Approach for Electrochemical Capacitors. *J. Electrochem. Soc.* **2006**, *153* (12), A2298. DOI: 10.1149/1.2359692
25. Chauhan, P.; Hiekel, K.; Diercks, J. S.; Herranz, J.; Saveleva, V. A.; Khavlyuk, P.; Eychmüller, A.; Schmidt, T. J. Electrochemical Surface Area Quantification, CO_2 Reduction Performance, and Stability Studies of Unsupported Three-Dimensional Au Aerogels versus Carbon-Supported Au Nanoparticles. *ACS Mater. Au* **2022**, *2* (3), 278–292. DOI: 10.1021/acsmaterialsau.1c00067
26. Röttcher, N. C.; Ku, Y.P.; Minichova, M.; Ehelebe, K.; Cherevko, S. Comparison of Methods to Determine Electrocatalysts' Surface Area in Gas Diffusion Electrode Setups: A Case Study on Pt/C and PtRu/C. *J. Phys. Energy* **2023**, *5* (2), 024007. DOI: 10.1088/2515-7655/acbe1b
27. Tackett, B. M.; Kimmel, Y. C.; Chen, J. G. Metal-Modified Niobium Carbides as Low-Cost and Impurity-Resistant Electrocatalysts for Hydrogen Evolution in Acidic and Alkaline Electrolytes. *Int. J. Hydrog. Energy* **2016**, *41* (14), 5948–5954. DOI: 10.1016/j.ijhydene.2016.01.167.

28. Sheng, W.; Myint, M.; G. Chen, J.; Yan, Y. Correlating the Hydrogen Evolution Reaction Activity in Alkaline Electrolytes with the Hydrogen Binding Energy on Monometallic Surfaces. *Energy Environ. Sci.* **2013**, *6* (5), 1509–1512. DOI: 10.1039/C3EE00045A
29. Anantharaj, S.; Karthik, P.E.; Noda, S. The Significance of Properly Reporting Turnover Frequency in Electrocatalysis Research. *Angew. Chem. Int. Ed.* **2021**, *60*, 23051-23067. DOI: 10.1002/anie.202110352
30. Lee, J. H.; Kattel, S.; Jiang, Z.; Xie, Z.; Yao, S.; Tackett, B. M.; Xu, W.; Marinkovic, N. S.; Chen, J. G. Tuning the Activity and Selectivity of Electroreduction of CO2 to Synthesis Gas Using Bimetallic Catalysts. *Nat. Commun.* **2019**, *10* (1), 3724. DOI: 10.1038/s41467-019-11352-0
31. Ravel, B.; Newville, M. ATHENA, ARTEMIS, HEPHAESTUS: Data Analysis for X-Ray Absorption Spectroscopy Using IFEFFIT. *J. Synchrotron Radiat.* **2005**, *12* (Pt 4), 537–541. DOI: 10.1107/S0909049505012719
32. Ravel, B.; Newville, M. ATHENA and ARTEMIS: Interactive Graphical Data Analysis Using IFEFFIT. *Phys. Scr.* **2005**, *2005* (T115), 1007. DOI: 10.1238/Physica.Topical.115a01007
33. Denny, S. R.; Tackett, B. M.; Tian, D.; Sasaki, K.; Chen, J. G. Exploring Electrocatalytic Stability and Activity of Unmodified and Platinum-Modified Tungsten and Niobium Nitrides. *Int. J. Hydrog. Energy* **2020**, *45* (43), 22883–22892. DOI: 10.1016/j.ijhydene.2020.06.186
34. Zhang, Q.; Jiang, Z.; Tackett, B. M.; Denny, S. R.; Tian, B.; Chen, X.; Wang, B.; Chen, J. G. Trends and Descriptors of Metal-Modified Transition Metal Carbides for Hydrogen Evolution in Alkaline Electrolyte. *ACS Catal.* **2019**, *9* (3), 2415–2422. DOI: 10.1021/acscatal.8b03990
35. Kresse, G.; Furthmüller, J. Efficiency of Ab-Initio Total Energy Calculations for Metals and Semiconductors Using a Plane-Wave Basis Set. *Comput. Mater. Sci.* **1996**, *6* (1), 15–50. DOI: 10.1016/0927-0256(96)00008-0.
36. Kresse, G.; Hafner, J. Ab Initio Molecular Dynamics for Open-Shell Transition Metals. *Phys. Rev. B* **1993**, *48* (17), 13115–13118. DOI: 10.1103/PhysRevB.48.13115